ACCEPTED

Thermal Analysis of Photodetectors in Steady-State

Ishraq Md Anjum,[1] Alexander S. Hastings,[2] David A. Tulchinsky,[2] Keith J. Williams,[2] Curtis R. Menyuk,[1] and Ergun Simsek[1,*]

[1] Department of Computer Science and Electrical Engineering, University of Maryland Baltimore County, Baltimore, MD 21250, USA

[2] U.S. Naval Research Laboratory, Washington, DC 20375 USA.

[*]simsek@umbc.edu

Abstract: This study introduces a method to approximate temperature distribution in steady-state photodetectors under optical excitation. Findings underscore the influence of temperature on key attributes, revealing overestimation with constant temperature assumptions. Insights aid in optimizing photodetector performance.

1. Introduction

Photodetectors (PDs), essential in microwave photonics [1–5], face challenges in realizing elevated RF output power due to saturation effects from the space-charge effect [1, 5] and heat-induced failure risks [6, 7]. Uni-traveling carrier (UTC) PDs address the space-charge effect, exhibiting enhanced high-power performance compared to traditional p-i-n PDs [8]. Modified uni-traveling carrier (MUTC) PDs, with a unique cliff layer controlling electric field strength, improve space-charge tolerance [2–4]. In [2], researchers noted increased responsivity in UTC and MUTC PDs due to elevated photoabsorption coefficient at higher temperatures. Despite progress, thermal challenges hinder achieving higher RF output power. This study explores thermal characteristics of backside-illuminated MUTC PDs, focusing on the MUTC2 variant [3], known for remarkable results, including a quantum efficiency of 0.55 and a bandwidth of 24 GHz [3]. A simple numerical model estimates temperature distribution, offering insights into temperature-dependent performance.

2. Numerical Model and Results

We solve drift-diffusion equations to study PDs [9, 10]. The heat transport equation, which describes the spatiotemporal dynamics of the temperature distribution in the photodetector, can be expressed as:

$$c_H \frac{\partial T}{\partial t} - \nabla \cdot \sigma_T \nabla T = H \qquad (1)$$

where T is the temperature, c_H represents the volumetric heat capacity, σ_T denotes the thermal conductivity, and H signifies the heat generation rate. If one aims to obtain an approximate temperature distribution for a photodetector in steady-state, Eq. (1) can be simplified into $-\nabla \cdot \sigma_T \nabla T = \mathbf{J} \cdot \mathbf{E}$, assuming that Joule heating is the primary heat source, where $\mathbf{E}$ and $\mathbf{J}$ represent the local electric field and current, respectively. When utilizing many thin layers, each with a thickness of δz to describe a layer of a semiconductor device (where $\delta z \ll \lambda$), this simplified expression indicates that the local temperature change in that thin layer can be approximated as $\nabla T \approx -(\mathbf{J} \cdot \mathbf{E})\delta z/\sigma_T$.

To validate our methodology, we performed a numerical investigation on the MUTC2. Initially assuming a constant 300 K temperature, we calculated local electric fields and currents at a -5 V reverse bias. We assumed a load resistance of 50 Ω. We used a non-uniform mesh [9] with a maximum grid spacing of 1 nm. Cumulatively summing these ∇T values, as shown in Fig. 1 (a), yielded an overall temperature change from the p-side to the n-side. Subsequently, we iteratively refined the temperature profile, stabilizing after the third iteration ($\Delta T_i < 10^{-3}$ °C). Electric field distributions (Fig. 1 (b)) revealed intense fields within the InGaAs absorber layers, leading to a significant temperature shift due to InGaAs's low thermal conductivity. Further analysis involved calculating temperature for varied optical excitations. The resultant temperature at the n-contact exhibited good agreement with measurement results (red circles) [4], validating our model, the blue curve in Fig. 1 (c).

Next, we investigated the impact of the approximate temperature distribution on the performance of the photodetector while it produces the same photocurrent as we allow the reverse bias to vary. The results are plotted in Fig. 2. The electric fields increasing with bias voltage accelerate the charge carriers, reducing their transit time through the photodetector. A reduced transit time spread leads to lower phase noise, as depicted in Fig. 2 (a). At

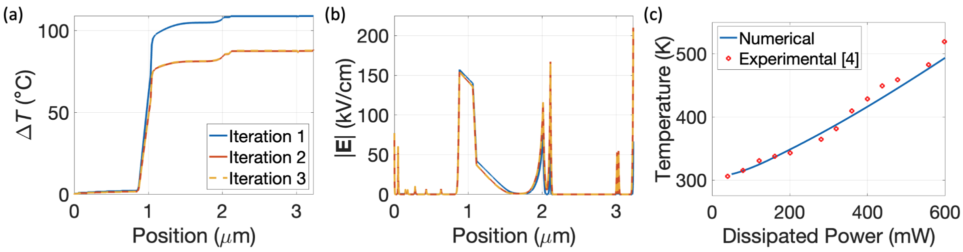

Fig. 1. (a) Temperature and (b) electric field distributions over the photodetector at the end of the first three iterations. (c) Temperature of the *n*-contact as a function of dissipated power.

high power levels, where the incident power is close to 1 W, the photodetector is close to a point where it becomes saturated, and additional incident photons do not result in a proportional increase in the generated electron-hole pairs, and hence the quantum efficiency saturates. The competing effects (narrowing bandgap and increasing carrier recombination) cause first an increase and then a decrease in the bandwidth with voltage, see Fig. 2 (c).

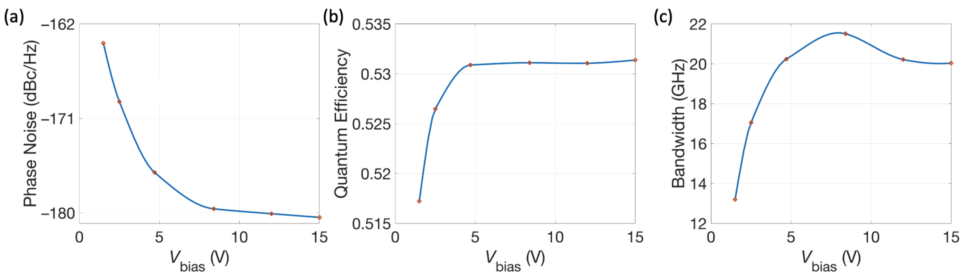

Fig. 2. (a) Phase noise, (b) quantum efficiency, and (c) bandwidth as a function of reverse bias voltage while the PD's output photocurrent is fixed at 40 mA.

3. Conclusions

This study introduces a simple yet effective method for approximating temperature distribution in photodetectors. Results highlight the importance of considering temperature variations in performance analysis, providing insights for optimization. The model, validated against experimental data, contributes to understanding thermal management in advanced photodetectors for high-power applications.

References

1. K. Williams, R. Esman, and M. Dagenais, "Effects of high space-charge fields on the response of microwave photodetectors," IEEE Photonics Technol. Lett. **6**, 639–641 (1994).
2. D.-H. Jun, J.-H. Jang, and J.-I. Song, "Effect of temperature on bandwidth and responsivity of uni-traveling-carrier and modified uni-traveling-carrier photodiodes," Jpn. J. Appl. Phys. **46**, 2360 (2007).
3. Z. Li, H. Pan, H. Chen, A. Beling, and J. C. Campbell, "High-saturation-current modified uni-traveling-carrier photodiode with cliff layer," IEEE J. Quantum Electron. **46**, 626–632 (2010).
4. Z. Li, Y. Fu, M. Piels, H. Pan, A. Beling, J. E. Bowers, and J. C. Campbell, "High-power high-linearity flip-chip bonded modified uni-traveling carrier photodiode," Opt. Express **19**, B385–B390 (2011).
5. N. Li, X. Li, S. Demiguel, X. Zheng, J. Campbell, D. Tulchinsky, K. Williams, T. Isshiki, G. Kinsey, and R. Sudharsansan, "High-saturation-current charge-compensated InGaAs-InP uni-traveling-carrier photodiode," IEEE Photonics Technol. Lett. **16**, 864–866 (2004).
6. K. Kato, "Ultrawide-band/high-frequency photodetectors," IEEE Trans. on Microw. Theory Tech. **47**, 1265–1281 (1999).
7. X. Wang, N. Duan, H. Chen, and J. C. Campbell, "InGaAs–InP photodiodes with high responsivity and high saturation power," IEEE Photonics Technol. Lett. **19**, 1272–1274 (2007).
8. T. Ishibashi, T. Furuta, H. Fushimi, S. Kodama, H. Ito, T. Nagatsuma, N. Shimizu, and Y. Miyamoto, "InP/InGaAs uni-traveling-carrier photodiodes," IEICE transactions on electronics **83**, 938–949 (2000).
9. E. Simsek, I. M. Anjum, and C. R. Menyuk, "Solving drift diffusion equations on non-uniform spatial and temporal domains," in *2023 Photonics & Electromagnetics Research Symposium (PIERS),* (2023), pp. 1644–1651.
10. E. Simsek, I. M. Anjum, T. F. Carruthers, C. R. Menyuk, J. C. Campbell, D. A. Tulchinsky, and K. J. Williams, "Fast evaluation of rf power spectrum of photodetectors with windowing functions," IEEE Trans. on Electron Devices **70**, 3643–3648 (2023).